Relationship between shortwave radiation bias over the Southern Ocean and the ITCZ in MRI-ESM2

Hideaki Kawai (h-kawai@mri-jma.go.jp), **Tsuyoshi Koshiro, and Seiji Yukimoto**
Meteorological Research Institute, JMA

1. Introduction

Kang et al. (2008, 2009) showed that the ITCZ responds to heating in the extratropics using a slab-ocean model and explained the mechanism in terms of the energy budget. Hwang and Frierson (2013) found relationships between the radiation bias over the Southern Ocean and the ITCZ in CMIP5 multi-models. Kay et al. (2016) and Hawcroft et al. (2017) used atmosphere–ocean coupled models to show that the excess energy in the Southern Ocean is transported to the Northern Hemisphere more by the ocean than by the atmosphere.

The previous version of the MRI climate model, MRI-CGCM3, which was used for CMIP5 simulations, had a serious negative bias in the reflection of shortwave radiation due to an unrealistically small cloud radiative effect (CRE) over the Southern Ocean. The negative bias was reduced significantly in MRI-ESM2 (Yukimoto et al. 2019), which is used in the CMIP6 simulations. The improvement is achieved by the accumulation of modifications in various physical schemes related to clouds (Kawai et al. 2019). Therefore, we can intentionally increase the shortwave radiation bias over the Southern Ocean by turning the modifications back to the old treatments one by one. By doing this, we can quantitatively examine the relationship between shortwave radiation bias over the Southern Ocean and the ITCZ in MRI-ESM2.

2. Experiments

The control run (CNTL) uses the standard version of MRI-ESM2 and has the smallest shortwave radiation bias over the Southern Ocean. In the simulation EXP1, the new stratocumulus scheme (Kawai et al. 2017, 2019) that can better reproduce stratocumulus is replaced by the old scheme (Kawai and Inoue 2006). In MRI-ESM2, the occurrence of shallow convection is prevented over the area where the conditions for stratocumulus occurrence are met. This has the effect of increasing marine stratocumulus. EXP2 is as EXP1, but the shallow convection conditional prevention is turned off. EXP3 is as EXP2, but the treatment of the Wegener–Bergeron–Findeisen process is turned from the new one that increases the ratio of supercooled liquid clouds to the old one. In MRI-ESM2, the number concentration of cloud condensation nuclei originating from fine mode sea salt is doubled to take into account the marine aerosols in the Aitken mode that cannot be explicitly represented in the model. EXP4 is as EXP3 but with the doubling (described above) that results in an increase in the optical depth of marine low clouds turned off. See Kawai et al. (2019) for more details related to these processes. These experiments are listed in Table 1 and the radiation bias is expected to monotonically increase from CNTL to EXP4. We ran the historical simulations with these five settings using the atmosphere–ocean coupled model. The models were run from 2000 to 2014, and data for the ten years from 2005 to 2014 were used for analysis.

3. Results

The left panel in Fig. 1 shows that the shortwave radiation flux at the top of the atmosphere (TOA) over the Southern Ocean increases monotonically (downward: positive) from CNTL to EXP4. The middle panel in Fig. 1 shows that the net (shortwave + longwave) radiation flux at the TOA also increases monotonically

	CNTL	EXP1	EXP2	EXP3	EXP4
stratocumulus scheme	new	old	old	old	old
shallow convection conditional turning off	yes	yes	no	no	no
WBF effect	new	new	new	old	old
fine sea aerosols	yes	yes	yes	yes	no

Table 1: List of settings for experiments.

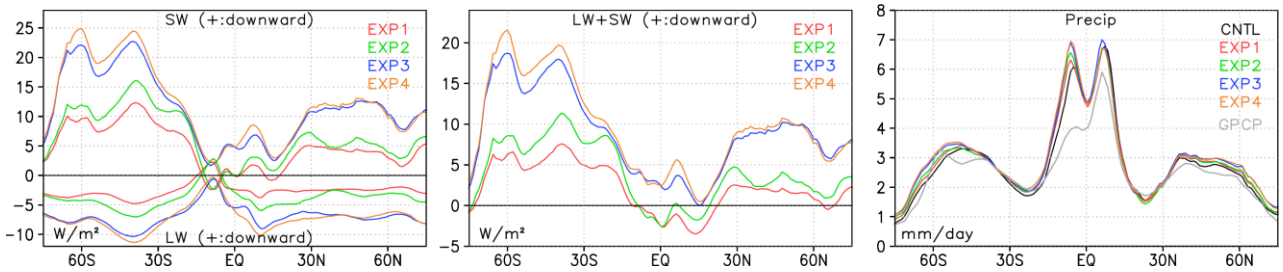

Fig. 1: Differences of shortwave and longwave radiative flux (left) and net (shortwave + longwave) radiative flux (middle) at TOA with respect to the control experiment for each experiment (unit: W/m^2, positive: downward). Precipitation (unit: mm/day) (right). Zonal means are plotted. MRI-ESM2 is used and the climatologies cover the period 2005–2014. GPCP observation period is 1979–2013.

from CNTL to EXP4, although the impact on shortwave radiation is partly compensated by the impact on longwave radiation. Actually, the impact on longwave radiation is caused more by the SST increase (i.e. clear sky radiation; ~70%) than changes in clouds (i.e. CRE; ~30%) (figure not shown). The right panel in Fig. 1 shows the impact on zonal mean precipitation. The peak in precipitation in the Southern tropics increases from CNTL to EXP4.

We calculated the asymmetry of extratropical radiative flux and CRE (Hwang and Frierson 2013), the tropical precipitation asymmetry index (Hwang and Frierson 2013), and the Southern ITCZ Index (Bellucci et al. 2010). Figure 2 shows clear relationships between the asymmetry of extratropical net radiative flux or CRE and tropical precipitation asymmetry or the Southern ITCZ Index. More extratropical radiative flux over the Southern Hemisphere than over the Northern Hemisphere corresponds to more tropical precipitation in the Southern Hemisphere than in the Northern Hemisphere or more precipitation over the Eastern Tropical Pacific in the Southern Hemisphere. Although the net (shortwave + longwave) radiation is used for the plots, the relationships essentially depend on the contribution of the shortwave component (figure not shown).

Figure 3 shows the impacts on energy transport relative to the control simulation. The impacts on the cross-equatorial northward energy transport are positive and the energy transport monotonically increases from CNTL to EXP4. The contribution of the ocean to the northward energy transport is almost twice the contribution of the atmosphere.

Although the change in transport by the ocean is larger than that by the atmosphere, as previous studies have shown, a clear relationship between the Southern Ocean radiation bias and ITCZ, as found by Hwang and Frierson (2013), is still seen in our simulations. It is possible that the alleviation of the double ITCZ problem in MRI-ESM2 compared to MRI-CGCM3 is partly attributable to the reduction of the Southern Ocean radiation bias.

Acknowledgements

This work was partly supported by the Integrated Research Program for Advancing Climate Models (TOUGOU) Grant Number JPMXD0717935561 from the Ministry of Education, Culture, Sports, Science and Technology (MEXT), Japan. It was also supported by the Japan Society for the Promotion of Science (JSPS) KAKENHI (Grant Nos. JP18H03363, JP19K03977, and JP19H05699), and the Environmental Restoration and Conservation Agency, Japan (the Environment Research and Technology Development Fund (Grant No. 2-2003)).

References

Bellucci, A., S. Gualdi, and A. Navarra, 2010: *J. Clim.*, **23**, 1127–1145.

Hawcroft, M., et al., 2017: *Clim. Dyn.*, **48**, 2279–2295.

Hwang, Y.-T., and D. M. W. Frierson, 2013: *Proc. Natl. Acad. Sci.*, **110**, 4935–4940.

Kang, S. M., et al., 2008: *J. Clim.*, **21**, 3521–3532.

Kang, S. M., D. M. W. Frierson, and I. M. Held, 2009: *J. Atmos. Sci.*, **66**, 2812–2827.

Kawai, H., and T. Inoue, 2006: *SOLA*, **2**, 17-20.

Kawai, H., T. Koshiro, and M. J. Webb, 2017: *J. Climate*, **30**, 9119-9131.

Kawai, H., et al., 2019: *Geosci. Model Dev.*, **12**, 2875–2897.

Kay, J. E., et al., 2016: *J. Clim.*, **29**, 4617–4636.

Yukimoto, S., et al., 2019: *J. Meteor. Soc. Japan*, **97**, 931–965.

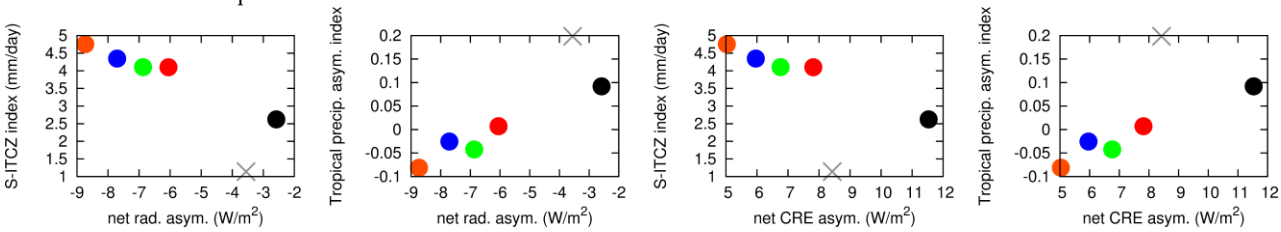

Fig. 2: Relationships between the asymmetry of extratropical net radiative flux or CRE and tropical precipitation asymmetry or the Southern ITCZ Index. The asymmetry of extratropical radiative flux or CRE is calculated as the average over 20°N–90°N minus that over 20°S–90°S (positive: downward, Hwang and Frierson 2013). The tropical precipitation asymmetry index is defined as the precipitation over 0°N–20°N minus that over 0°S–20°S normalized by the total tropical precipitation (20°S–20°N) (Hwang and Frierson 2013). The Southern ITCZ Index (mm/day) is defined as the annual mean precipitation over the 20°S–0°S, 100°W–150°W window (Bellucci et al. 2010). Crosses denote observations: CERES (2001–2010) for radiative flux and CRE, and GPCP (1979–2013) for precipitation. These plots use the same data as Fig. 1 and the colors of the symbols are shown in the panels in Fig. 1.

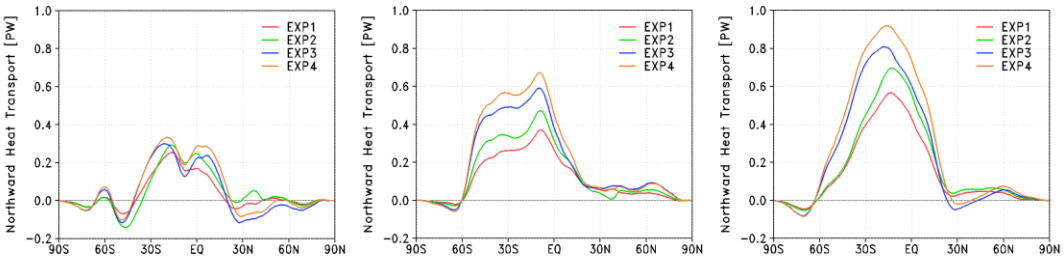

Fig. 3: Differences of northward heat transport by the atmosphere (left), the ocean (middle), and the sum (right) with respect to the control experiment (unit: PW). These plots use the same data as Fig. 1.